Using Image Processing and Automated Classification Models to Classify Microscopic Gram Stain Images

Kristensen, Kris; Ward, Logan Morgan; Mogensen, Mads Lause; Cichosz, Simon Lebech

Published in:
Computer Methods and Programs in Biomedicine Update

DOI (link to publication from Publisher):
10.1016/j.cmpbup.2022.100091

Publication date:
2023

Document Version
Publisher's PDF, also known as Version of record

Computer Methods and Programs in Biomedicine Update 3 (2023) 100091

Contents lists available at ScienceDirect

Computer Methods and Programs in Biomedicine Update

journal homepage: www.sciencedirect.com/journal/computer-methods-and-programs-in-biomedicine-update

Using image processing and automated classification models to classify microscopic gram stain images

Kris Kristensen [a], Logan Morgan Ward [b], Mads Lause Mogensen [b], Simon Lebech Cichosz [a,*]

[a] Department of Health Science and Technology, Aalborg University, Denmark
[b] Treat Systems, Aalborg, Denmark

ARTICLE INFO

Keywords:
Gram stain
Blood culture
Machine learning
Deep learning
Automated microscopy
Analytics
Artificial intelligence
Automation

ABSTRACT

Background and Objective: Fast and correct classification of bacterial samples are important for accurate diagnostics and treatment. Manual microscopic interpretation of Gram stain samples is both time consuming and operator dependent. The aim of this study was to investigate the potential for developing an automated algorithm for the classification of microscopic Gram stain images.

Methods: We developed and tested two algorithms (using image processing an Casual Probabilistic Network (CPN) and a Random Forest (RF) classification) for the automated classification of Gram stain images. A dataset of 660 images including 33 microbial species (32 bacteria and one fungus) was split into training, validation, and test sets. The algorithms were evaluated based on their ability to correctly classify samples and general characteristics such as aggregation and morphology.

Results: The CPN correctly classified 633/792 images to achieve an overall accuracy of 80% compared to the RF which correctly classified 782/792 images to achieve an overall accuracy of 99% ($p < 0.001$). The CPN performed well when distinguishing between GN and GP, with an accuracy of 95% (731/768). The RF also performed well in distinguishing between GN and GP, achieving an accuracy of 99% (767/768) ($p < 0.001$).

Conclusions: The findings from this study show promising results regarding the potential for an automated algorithm for the classification of microscopic Gram stain images.

1. Introduction

Infectious diseases are a major cause of public health concern. Infections account for more than 11% of all deaths worldwide, corresponding to 6.7 million deaths each year [1]. Antibiotics are used as medical treatment for bacterial and fungal infections, which has saved countless lives since their discovery in 1928 [2]. Over time, pathogens develop resistance to antibiotic treatment, with some resistant strains becoming increasingly difficult or almost impossible to treat [3,4]. Resistant pathogens are a major threat to global health [5]. A total of 2.8 million Americans are affected by resistant pathogens each year. The resistant pathogens cause 35,000 deaths in the USA and 33,000 in Europe annually [6,7].

The leading cause of bacterial resistance is the unnecessary use of broad-spectrum antibiotics [8]. Broad-spectrum refers to the activity of the drugs across a range of bacterial species, and because of this, these drugs are often used for empirical antibiotic therapy before the causative pathogen has been identified. In contrast, narrow-spectrum antibiotics do not stimulate the growth of antibiotic resistance connected with the use of broad-spectrum antibiotics. However, before using narrow-spectrum antibiotics, identification of the bacterial species is required to ensure that the correct drug is selected to cover the specific causative pathogen [9].

The standard method of identifying bacterial species is a sequential procedure including extraction of blood cultures, incubation, Gram staining, microscopic examination and sometimes gene-sequencing and susceptibility testing [9]. The second part of the procedure relies exclusively upon manual labor, which can cause both increased time-to-result and errors [10].

In microbiology, Gram staining is a method of staining used to classify bacterial species into two large groups: (A) gram-positive bacteria and (B) gram-negative bacteria. Gram staining distinguishes bacteria by the chemical and physical properties of their cell walls. gram-positive bacteria have a thicker layer of peptidoglycan (a polysaccharide) in the cell wall that preserves the primary stain, crystal violet. gram-negative cells have a thin layer that allows the color to wash

* Corresponding author at: Fredrik Bajers Vej 7D2 - DK-9220 Aalborg, Denmark.
E-mail address: simcich@hst.aau.dk (S.L. Cichosz).

https://doi.org/10.1016/j.cmpbup.2022.100091
Received 25 November 2021; Received in revised form 30 November 2022; Accepted 29 December 2022
Available online 30 December 2022

out upon addition of ethanol in the staining procedure. gram-negative cells are stained pink or red by the counterstain. The interpretation of the Gram stain color is manually examined under a microscope; in addition to the Gram stain color, several bacterial characteristics are assessed (such as aggregation of bacteria, morphology, and size) to classify the sample [11].

Gene sequencing is becoming a widely used technique in clinical diagnosis. It enables the precise characterization of bacteria in terms of its properties, including antibiotic resistance, molecular epidemiology, and virulence [12].

Examples of these time-consuming aspects can be numerous. A natural reason for time delay can be that samples are postponed until a batch of the sample is ready [10]. Other reasons could be working schedules, i.e., closed laboratory at night or specific microbiologists are on break. Despite experienced staff, manual labor still contributes significantly to additional time to result [13]. Furthermore, in addition to the time-consuming aspects of manual labor, classification errors also occur [13]. A study by Guarner et al. [13] tested 23 medical laboratory scientists in the classification of Gram stain samples. The scientists classified 71–77% of the samples correctly in relation to Gram stain color and 53–66% correctly in relation to morphology and aggregation. A solution to decrease the time-to-result and reduce the number of errors during the identification procedure could be to eliminate time-consuming manual labor by automating the classification process [14]. In other medical domains, image analysis and machine learning algorithms have shown great potential for improving diagnostics and treatment [15–19].

The aim of this study was to investigate the potential for developing an automated algorithm for the classification of microscopic Gram stain images.

2. Methods

To investigate the potential for an automated classification of microscopic Gram stain images, we developed and tested two algorithms based on image analysis and machine learning. Both algorithms utilized the same image processing, but different machine learning models were assessed for their ability to correctly classify the images. The development process for the two algorithms is illustrated in Fig. 1.

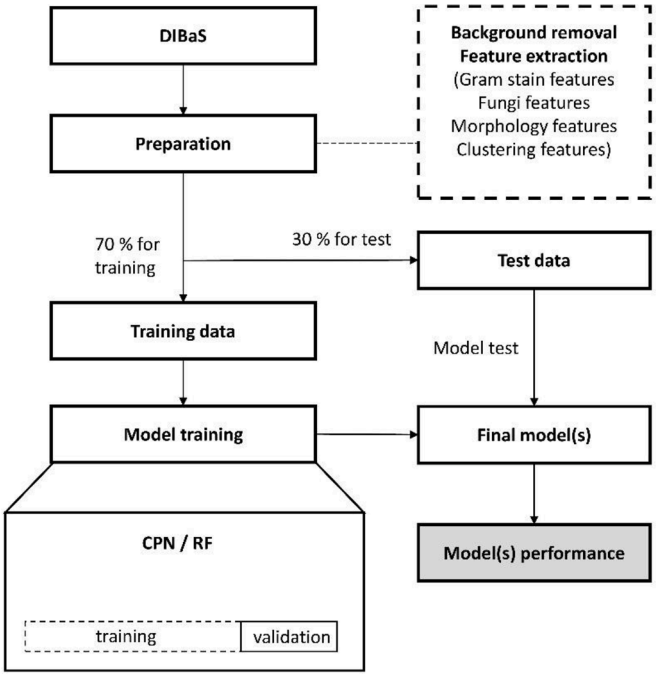

Fig. 1. Flowchart of steps involved in the development of the algorithms for classification of Gram stain images.

The first machine learning model chosen was a causal probabilistic network (CPN) that utilizes conditional probabilities in the classification. By using conditional probabilities, this method includes a high level of transparency and self-explanatory to the user[20].

The second machine learning method was a data-driven machine learning approach called random forest. The random forest model typically operates with higher accuracy than simpler models. The disadvantage of random forest is that the reasoning behind the result is more complex to interpret [21].

All image processing and the random forest were implemented using MATLAB R2020b (The Mathworks Inc., Natick, Massachusetts), and the CPN was implemented using Hugin (Hugin Expert A/S, Gasværksvej 5, DK-9000 Aalborg, Denmark).

2.1. Data acquisition and preparation

We utilized data from the Digital Images of Bacteria Species dataset (DIBaS) [22]. DIBaS is a publicly available database and contains 660 microscopic Gram stain images. The 660 images are distributed evenly between 33 microbial species (32 bacteria and one fungus). All images were collected by Jagiellonian University in Krakow, Poland. All images were stained by Gram's method [23] using the same equipment under equal conditions. The equipment used was an Olympus CX31 Upright Biological Microscope equipped with an SC30 camera (Olympus Corporation, Japan). They were evaluated using a 100 times objective under oil immersion (Nikon50, Japan)[23]. Photo example of different species are presented in the *supplementary material table s2*.

The 660 images in DIBaS were split into training (50%), validation (20%) and test (30%) sets, stratifying the split according to the 33 species to ensure that the same class balance was maintained across the splits.

All images in DIBaS have the same dimensions of 1532 × 2048 pixels. The images are of high quality, and they contain sufficient detail that information is retained on division into smaller images. The images were divided into four equal quarters of 766 × 1024 pixels to increase the number of images for training and test purposes[23] without compromising the quality of the images. The division of images resulted in a training set of 1320 images with an even distribution across the 33 species; likewise, there was a validation set of 528 images and a test set of 792 images.

The training and validation datasets were used to train the two machine learning models and optimize the performance, while the test dataset was used for the final evaluation of the models' performance. This procedure ensured that the results were not prone to overfitting and would be transferable to a similar cohort using the same type of images [24].

2.2. Background removal

We used Otsu's method to remove the background of each image after transforming the images to grayscale. The strength of Otsu's method in simple images is the use of a global threshold. OTSU's method uses interclass variance between the foreground and background to determine the best threshold to distinguish foreground and background [25]. An example of the use of this method to remove the background of the images is shown in Fig. 2.

2.3. Feature extraction

When classifying Gram stain images, microbiologists look for different bacterial characteristics, such as Gram stain color, morphology, sizes, and aggregation. The characteristics are used to classify samples into broad categories: gram-negative (GN), gram-positive (GP) (with subcategories: Staphylococcus, Streptococcus, other GP) and fungi[26]. The same characteristics are used in the

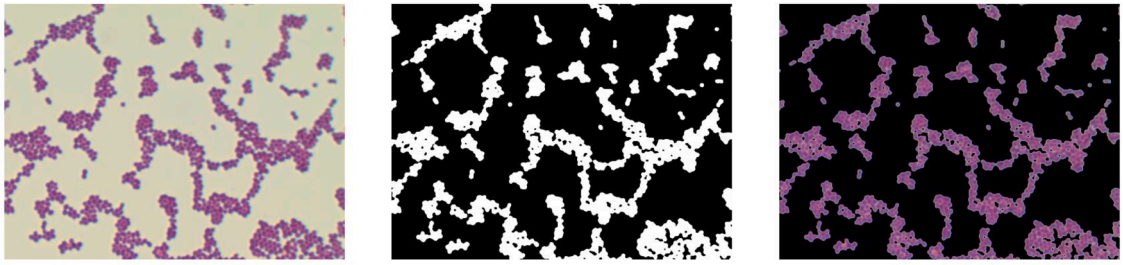

Fig. 2. Illustrations of how the original image (a) is binarized (b) and then multiplied with the original images, resulting in background removal (c).

algorithms to classify the images. These image features are extracted in several steps. An overview of all features is presented in *supplementary material table s1*.

2.3.1. Gram stain and fungal features (color features)

Gram stain color features were extracted from the images after removal of the background. A total of 12 features were extracted from each image to help determine whether the bacteria were gram-positive or gram-negative. The color features are important to separate bacterial samples from samples with fungi.

Each image pixel consists of red, green, and blue color intensities in the range 0 to 255. A median value of these intensities is calculated, resulting in one feature for each of the three colors. Furthermore, color spectra of the images are used to calculate features. An example of the color spectra for gram-negative and gram-positive bacteria is presented in *supplement material figure s1*.

The highest color intensity peak is used for red, green, and blue color. Another feature from the color spectrum extracted is the magnitude of the colors below an intensity of 200; the threshold chosen by visual inspection of the color spectrum. The final set of color features used enhancement of the colors in the images as described by Zuiderveld [27]. The enhanced median colors (red, green, and blue) were extracted as features.

2.3.2. Morphology features

Morphology features were extracted to distinguish between different bacterial species. In this study, two shapes were used to distinguish the morphology of bacteria: cocci and bacilli. Cocci have a round shape, and bacilli have a rod shape[26]. An example of a bacillus and a coccus is illustrated in Fig. 3. To classify whether a bacterium is round or rod shaped, the individual bacteria must be isolated. Isolated bacteria were defined by an 8-connectivity method. 8-connectivity defines clusters if pixels are connected in any direction. An erosion operation followed by a dilation was used on the binary images after background removal and prior to the individual bacterial extraction. Erosion shrinks the isolated bacteria, and dilation dilates the isolated bacteria. A combination of these operations results in smoother edges of the isolated bacteria and removes small pixel groups [28]. A comparison between the original image and the processed image used for the isolation of bacteria is presented in *Supplemental Figure s2*. The individual segmentation of bacteria was not perfect but provided an average estimate of the morphology in the Gram-stained images.

After the isolation of the bacteria, features describing the shape were extracted. The extracted features were circularity, eccentricity, and roundness.

Circularity is calculated as (A = area; P = perimeter):

$$Circularity = \frac{4 \cdot A \cdot \pi}{P^2}$$

The eccentricity is calculated as a ratio of the distance between the major axis of the ellipse and the center of the bacteria (a = major axis length of ellipse; b = minor axis length of ellipse). This formula is an expression of eccentricity, which describes how elongated the isolated bacteria were. An eccentricity of 0 equals a circle, while an eccentricity of 1 equals a straight line:

$$Eccentricity = \frac{2\sqrt{\left(\frac{a}{2}\right)^2 - \left(\frac{b}{2}\right)^2}}{a}$$

The last feature used to express the shape is a roundness feature, expressed by the ratio between the length and the width of the bacteria. A perfect circle would have the same length and width and thereby result in a ratio of 1, whereas bacilli would have a longer length than width, and the ratio tends toward 0:

$$Roundness = \frac{w}{l}$$

These morphological features are calculated for every isolated bacterium in the image. The image is then described using the mean of each feature across all the isolated bacteria.

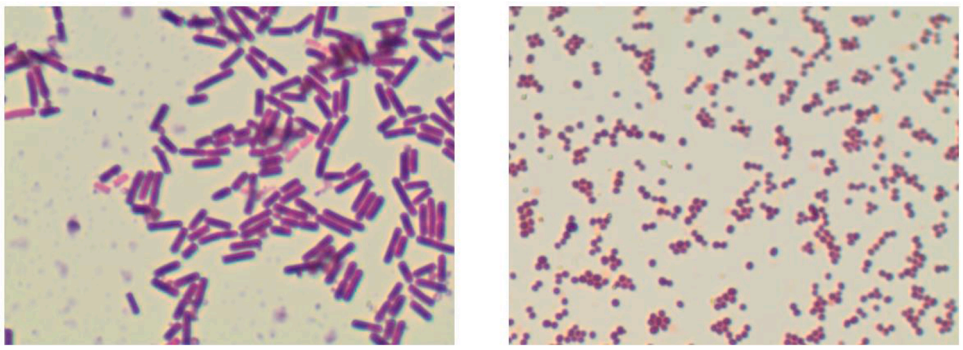

Fig. 3. Illustrations of the shape difference between bacilli (a) and cocci (b) bacteria.

2.3.3. Aggregation features

Aggregation is particularly relevant for GP cocci, which can be aggregated in three different ways. The aggregation is either in chains, in grape-like groups, or in singles[26]. In Fig. 4, the three GP cocci aggregations are shown. To extract aggregation features, the images are preprocessed further. The preprocessing includes background removal, finding bacteria and defining clusters. *Figure s3 in the Supplementary material* illustrates the transformation of the original image into a binary image of clusters.

After background removal, an image processing technique named watershed was used to separate the connected bacteria [29]. After separation of the bacteria, the centers of the bacteria were found. The Euclidean distance between all centers was calculated and gathered in a distance matrix. The distances were used to define aggregated bacteria. Bacteria with a Euclidean distance shorter than a threshold of 20 pixels were defined as aggregated. The threshold was determined empirically from the training data. The aggregated bacteria were then merged into clusters. The features used to define the type of aggregation were extracted from these clusters. For every cluster, ten features were extracted: mean cluster area, number of aggregated bacteria within each cluster, cluster density (number of aggregated bacteria divided by area), mean circularity of cluster, mean eccentricity of cluster, mean length of cluster, mean width of cluster, mean length divided by width, mean distance between clusters, and number of clusters containing three or fewer bacteria.

2.4. Classification models

Two classification models (CPN and random forest) were trained and optimized on the training and validation datasets. The test dataset was applied to the finalized models.

2.4.1. Causal probabilistic network

CPNs are a family of graphical models that can be drawn as directed acyclic graphs and consist of two main elements, nodes representing variables and arrows representing the causal links between the variables. The structure of the graph defines a set of conditional probability tables that describe the relationships between variables. The relationship between parent and child nodes is represented as conditional probability [30]. Conditional probability can be calculated using the formula:

$$P(A|B) = \frac{P(A|B)\cdot P(A)}{P(B)}$$

$P(A|B)$ = *posterior probability*
$P(B|A)$ = *likelihood probability*
$P(A)$ = *prior probability*

The probabilistic network approach was chosen due to the transparency of the network, as it can be designed to imitate the current workflow of microbiologists [31]. In this way, the model and the classification could be easier to understand for microbiologists compared to more complex classification models.

In this study, the CPN structure was specified manually. The structure consisted of three levels of nodes: a set of leaf nodes (level 3) representing the features extracted from the images; a set of nodes representing latent variables (level 2) gram stain, fungi, morphology, and aggregation; and the classification node (level 1) named *result*. Hugin (Hugin Expert A/S, Gasværksvej 5, DK-9000 Aalborg, Denmark) was used to specify the CPN structure. The conditional probability tables were learned from the training data using Hugin's EM learning algorithm. EM (expectation maximization) is a maximum-likelihood method that iteratively adjusts the conditional probability tables to maximize the joint probability of the evidence across all learning cases. The graphical representation of the implemented CPN is presented in *supplementary material figure s4*.

2.4.2. Random forest

In contrast to the transparency of the probabilistic network, we also trained and tested a model based on random forest. The idea was to test whether performance could be increased by using a data-driven classification approach. The hyperparameters were optimized regarding performance and transferability using the training/validation split of the data. The random forest was optimized using the training/validation dataset to find the best number of trees in the range of 1–100. The number of learning cycles and the leaf size were chosen empirically.

2.5. Model evaluation

Both classification models were evaluated using confusion matrices with precision and accuracy. Images were classified as the class with the highest probability output from the models. Differences in accuracy were assessed using the chi-squared test.

3. Results

The confusion matrix for the model's performance is shown in Table 1. The samples were classified as GN (216), GP-other (408), GP-Strep (72), GP-Staph (72), or fungi (24). A total of 792 images were tested.

The CPN correctly classified 633/792 images to achieve an overall accuracy of 80% on the test set. However, only 13/72 (18%) of GP-Staph samples and 11/72 (15%) of GP-Strep samples were classified correctly, with the remainder classified as GP-other.

The CPN performed better when distinguishing between GN and GP, with an accuracy of 95% (731/768).

The random forest model performed significantly better than the CPN, correctly classifying 782/792 images to achieve an overall accuracy of 99% on the test set. Notably, the RF correctly classified 65/72 (89%) of GP-Staph samples and 72/72 (100%) of GP-Strep.

The RF performed well in distinguishing between GN and GP, achieving an accuracy of 99% (767/768). All accuracies were significantly[32] higher than those of the Casual Probabilistic Network ($p <$

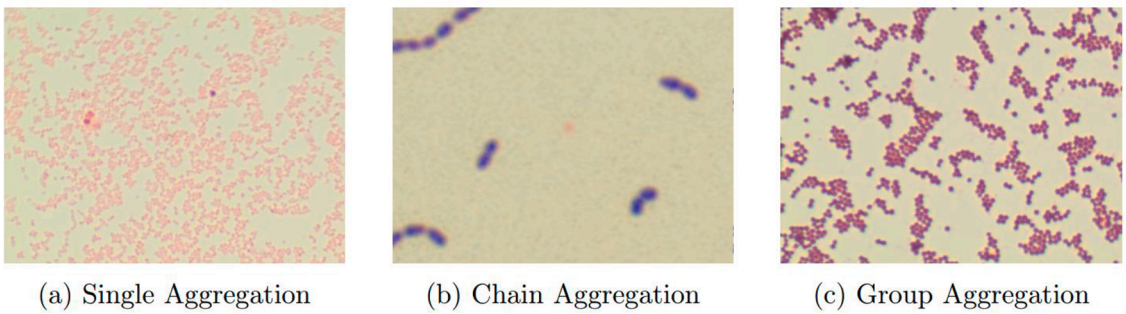

Fig. 4. Illustration of the different types of aggregation considered: single aggregation (a), chain aggregation (b) and group aggregation (c).

Table 1
Confusion matrix of the model performance. (Top) Casual Probabilistic Network and (bottom) Random Forest for the test dataset.

Casual Probabilistic Network		Predicted					
		Gram neg	Gram pos	Streptococcus	Staphylococcus	Fungi	Sensitivity [%]
True	Gram neg	194	22	0	0	0	90
	Gram pos	15	393	0	0	0	96
	Streptococcus	0	61	11	0	0	15
	Staphylococcus	0	59	0	13	0	18
	Fungi	0	2	0	0	22	92
	Precision [%]	93	73	100	100	100	**Accuracy [%] 80**
Random Forest		**Predicted**					
		Gram neg	Gram pos	Streptococcus	Staphylococcus	Fungi	Sensitivity [%]
True	Gram neg	215	1	0	0	0	100
	Gram pos	0	407	1	0	0	100
	Streptococcus	0	0	72	0	0	100
	Staphylococcus	0	5	3	64	0	89
	Fungi	0	0	0	0	24	100
	Precision [%]	100	99	95	100	100	**Accuracy [%] 99**

0.001).

4. Discussion

The aim of this study was to investigate the potential for developing an automated algorithm for the classification of microscopic Gram stain images. Two algorithms were presented, one with high transparency (Casual Probabilistic Network) and one focused on high performance (Random Forest). The overall accuracy for the causal probabilistic network was 80%, and for the random forest model, the accuracy was 99%. These accuracies are considered strong and indicate that a high percentage of images are classified correctly.

These results should be compared to manual interpretation, which is currently the standard for assessing Gram stain samples. Two studies by Sandle and Samuel et al. [33,34] evaluated the performance of microbiologists in determining Gram stain color. The microbiologists successfully classified the Gram stain color correctly in 92–97% [33,34]. In this study, the causal probabilistic network and the random forest performed similarly on this task, with accuracies of 95% and 99%, respectively.

A study by Guarner et al. [35] tested the ability of hospital personnel to determine the aggregation of samples. Laboratory scientists at the hospital trained in microbiology had a success rate of 53–66% without routine practice. After training and routine practice, the success rate increased to 73–96% [35]. The causal probabilistic network performed poorly in distinguishing between aggregations, as evidenced by the high rate of misclassification within the wider GP group, with GP-Strep and GP-Staph wrongly classified as GP-other. However, our results indicate that the random forest model may outperform laboratory scientists, achieving an accuracy of 97% in the present study.

Several articles on automated bacterial classifications using machine learning have been published in the last decade [36]. The results are promising on different aspects of automated classification [36–39].

Zieliński et al. [22] reported on the usage of deep convolutional neural networks to obtain image descriptors, with subsequent encoding and classification with support vector machine or random forest. The approach was based on the DIBaS dataset and had an accuracy of up to 97%.

In a similar study of automated models, Smith et al. [35] used a similar methodical approach that was comparable to ours. The study by Smith et al. used a deep convolutional neural network to classify microscopic Gram stain images into gram-negative, gram-positive, gram-positive chains and gram-positive clusters, which are equivalent to the labels used in this study. The deep convolutional neural network showed an overall accuracy of 93%.

Additionally, Zawadzki et al. [40] presented several deep learning approaches to the classification of selected fungi and bacteria with accuracies between 96–100% in three datasets. Zieliński et al. [41] also recently reported a deep learning approach to describe and classify microscopic fungal images. Another approach was reported by Yang et al. on a method on automated tuberculosis classification in Ziehl-Neelsen stained slides [39].

Both models proposed in this study showed promising results compared to manual classification and existing models. Compared to previous studies the results show that a feature-based learning approach could also be used with high accuracy in classifying bacteria from gram-stain images compared to a deep learning approach reported by previous studies. Feature-based learning could potentially have an advantage in designing a transparent decision-support system for aiding microbiologists in microbial classification. Appropriate prescription of antibiotics is important to reduce one of the main drivers behind bacterial resistance. The results show that automated classification algorithms could potentially decrease the number of interpretation errors made by manual interpretation. In addition to minimizing errors, the operational time can also be decreased. The time delay caused by manual work [10,13] could be reduced by an automated system, which could potentially lead to faster diagnostics and treatment.

The proposed causal probabilistic network performed with significantly lower accuracy than the random forest model. However, with its high accuracy on the test set, the random forest model proved that the information is captured by the features. From a future perspective, it could be interesting to further investigate whether it is possible to optimize or reconstruct the causal probabilistic network to match the performance of the random forest model. An optimized causal probabilistic network could enable both high performance and high transparency.

4.1. Strengths and limitations

One advantage of the data used in this study is that all bacterial samples are stained with the same method, and the images are taken under the same conditions with the same type of equipment. Along with the many images comes significant diversity. The dataset includes 33 different bacterial species, which are representative of the most common bacterial species. In addition, the amount and quality of the data contribute to model robustness. The sample includes bacterial shapes classified as either cocci or bacilli. However, in clinical practice, several other shapes would need to be considered to cover a broader range of different species.

However, the robustness of the models is not tested under different settings, as all image samples are collected at the same hospital. Other hospitals might use other techniques, with different color intensities and image zoom levels. For instance, part of the proposed image analysis feature extraction is reliant on pixel-based distances, which are sensitive to the zoom level of the image.

Technical setup aspects relating to the image capture equipment

have not been included in this study. However, this is a pragmatic limitation only, as implementation of a fully automated system could potentially determine the specification for the equipment and procedure that should be used to obtain the Gram stain images.

Another limitation of the data is the low representation of fungi. Of the 33 microbial species, only a single fungal species was represented. The low representation of fungi creates uncertainty in the model's performance in the classification of fungi. The models classify fungi by their color difference in relation to bacteria. Different fungal species could mean different colors or other characteristics, causing the model to potentially struggle in classifying these other species. This limitation of species representation in the dataset also transfers to bacterial species. In future work, inclusion of a wider range of relevant bacterial species should be a priority. Additionally, including an "unknown" outcome prediction in the models could be of clinical relevance for a decision support system, where expert microbiologists could be involved in difficult cases where the automated system is unsure.

5. Conclusions

The findings from this study show promising results regarding the potential for an automated algorithm for the classification of microscopic Gram stain images. However, the algorithms proposed in this study need to be validated on a large dataset of heterogeneous samples to ensure robustness.

Author contributions

KK had access to all the data analyzed in this study and performed the statistical analysis. KK, LMW, MLM, and SLC take responsibility for the integrity and the accuracy of the study data analysis and results. KK, MLM, LMW, and SLC were involved in the study design, concept, analysis, and interpretation of data. SLC and KK drafted the manuscript. MLM and LMW were involved in critical revision of the manuscript

Funding received

None to disclose

Declaration of Competing Interest

MLM and LMW are employees of Treat Systems (Hasserisvej 125, 9000 Aalborg, DK)

Acknowledgements

None

Supplementary materials

Supplementary material associated with this article can be found, in the online version, at doi:10.1016/j.cmpbup.2022.100091.

References

[1] World Health Organization, WHO - The top 10 Causes of Death, WHO, 2020. PublishedAccessed July 2, 2021, https://www.who.int/news-room/fact-sheets/detail/the-top-10-causes-of-death.
[2] S. Aldrigde, The Discovery and Development of Penicillin 1928-1945, American Chemical Society, 1999. PublishedAccessed July 2, 2021, https://www.worldcat.org/title/discovery-and-development-of-penicillin-1928-1945-the-alexander-fleming-laboratory-museum-london-uk-november-19-1999-an-international-historic-chemical-landmark/oclc/43722822.
[3] H.D. Marston, D.M. Dixon, J.M. Knisely, T.N. Palmore, A.S. Fauci, Antimicrobial resistance, JAMA - J. Am. Med. Assoc. 316 (11) (2016) 1193–1204, https://doi.org/10.1001/jama.2016.11764.
[4] R. Wise, T. Hart, O. Cars, et al., Antimicrobial resistance, Br. Med. J. 317 (7159) (1998) 609–610, https://doi.org/10.1136/bmj.317.7159.609.
[5] World Health Organization, Antimicrobial Resistance - global report On Surveillance, World Health Organization, 2014, pp. 383–394, 61(3).
[6] US Department of Health and Human Services, CDC. Antibiotic resistance threats in the United States. Centers for Disease Control and Prevention. doi:10.15620/cdc:82532.
[7] A. Cassini, L.D. Högberg, D. Plachouras, et al., Attributable deaths and disability-adjusted life-years caused by infections with antibiotic-resistant bacteria in the EU and the European economic area in 2015: a population-level modelling analysis, Lancet Infect. Dis. 19 (1) (2019) 56–66, https://doi.org/10.1016/S1473-3099(18)30605-4.
[8] A.E. Paharik, H.L. Schreiber, C.N. Spaulding, K.W. Dodson, S.J. Hultgren, Narrowing the spectrum: the new frontier of precision antimicrobials, Genome Med. 9 (1) (2017) 1–4, https://doi.org/10.1186/s13073-017-0504-3.
[9] S. Leekha, C.L. Terrell, R.S. Edson, General principles of antimicrobial therapy, in: Mayo Clinic Proceedings, 86, Elsevier Ltd, 2011, pp. 156–167, https://doi.org/10.4065/mcp.2010.0639.
[10] O. Dauwalder, L. Landrieve, F. Laurent, M. de Montclos, F. Vandenesch, G. Lina, Does bacteriology laboratory automation reduce time to results and increase quality management? Clin. Microbiol. Infect. 22 (3) (2016) 236–243, https://doi.org/10.1016/j.cmi.2015.10.037.
[11] J. Vandepitte, J. Verhaegen, K. Engbaek, P. Rohner, P. Piot, C.C. Heuck, Basic Laboratory Procedures in Clinical Bacteriology, World Health Organization, November 24, 2022. Published online 2003:20. Accessed, https://books.google.com/books/about/Basic_Laboratory_Procedures_in_Clinical.html?hl=da&id=UHY0DgAAQBAJ.
[12] O. Opota, A. Croxatto, G. Prod'hom, G. Greub, Blood culture-based diagnosis of bacteraemia: state of the art, Clin. Microbiol. Infect. 21 (4) (2015) 313–322, https://doi.org/10.1016/j.cmi.2015.01.003.
[13] Q. Choi, H.J. Kim, J.W. Kim, G.C. Kwon, S.H. Koo, Manual versus automated streaking system in clinical microbiology laboratory: performance evaluation of Previ Isola for blood culture and body fluid samples, J. Clin. Lab. Anal. 32 (5) (2018), https://doi.org/10.1002/jcla.22373.
[14] R.B. Thomson, E. McElvania, Total laboratory automation: what is gained, what is lost, and who can afford it? Clin. Lab Med. 39 (3) (2019) 371–389, https://doi.org/10.1016/j.cll.2019.05.002.
[15] S.L. Cichosz, M.D. Johansen, O. Hejlesen, Toward big data analytics: review of predictive models in management of diabetes and its complications, J. Diabetes Sci. Technol. 10 (1) (2016) 27–34, https://doi.org/10.1177/1932296815611680.
[16] K.P. Smith, J.E. Kirby, Image analysis and artificial intelligence in infectious disease diagnostics, Clin. Microbiol. Infect. 26 (10) (2020) 1318–1323, https://doi.org/10.1016/j.cmi.2020.03.012.
[17] L. Mulrane, E. Rexhepaj, S. Penney, J.J. Callanan, W.M. Gallagher, Automated image analysis in histopathology: a valuable tool in medical diagnostics, Expert Rev. Mol. Diagn. 8 (6) (2008) 707–725, https://doi.org/10.1586/14737159.8.6.707.
[18] S.L. Cichosz, M.H. Jensen, O. Hejlesen, Short-term prediction of future continuous glucose monitoring readings in type 1 diabetes: development and validation of a neural network regression model, Int. J. Med. Inform 151 (2021), 104472, https://doi.org/10.1016/J.IJMEDINF.2021.104472.
[19] S.L. Cichosz, N.H. Rasmussen, P. Vestergaard, O. Hejlesen, Precise prediction of total body lean and fat mass from anthropometric and demographic data: development and validation of neural network models, J. Diabetes Sci. Technol. 15 (6) (2020) 1337–1343, https://doi.org/10.1177/1932296820971348.
[20] Andreassen S. *Medical decision support systems based on causal probabilistic networks*. 2000.
[21] J. Krause, A. Perer, K. Ng, Interacting with predictions: visual inspection of black-box machine learning models, in: Conference on Human Factors in Computing Systems - Proceedings, May 7, 2016, pp. 5686–5697, https://doi.org/10.1145/2858036.2858529. Published online.
[22] B. Zieliński, A. Plichta, K. Misztal, P. Spurek, M. Brzychczy-Włoch, D. Ochońska, Deep learning approach to bacterial colony classification, PLoS ONE 12 (9) (2017), e0184554, https://doi.org/10.1371/JOURNAL.PONE.0184554.
[23] S. Ann, H. Marise, Gram Stain Protocols | ASM.org, American Society for Microbiology, 2019. PublishedAccessed August 2, 2021, www.asmscience.org.
[24] Kohavi R. *A study of cross-validation and bootstrap for accuracy estimation and model selection.*; 1995.
[25] D. Liu, J. Yu, Otsu method and K-means, in: Proceedings - 2009 9th International Conference on Hybrid Intelligent Systems 1, HIS, 2009, pp. 344–349, https://doi.org/10.1109/HIS.2009.74, 2009.
[26] J. Topsall, Basic laboratory procedures in clinical bacteriology, Pathology 24 (4) (1992) 321, https://doi.org/10.1016/s0031-3025(16)35813-5.
[27] K. Zuiderveld, Contrast Limited Adaptive Histograph Equalization, Academic Press Professional, Graphic Gems IV San Diego, 1994, pp. 474–485. Published online.
[28] Parker J.R. (Jim R.), Terzidis K. Algorithms for image processing and computer vision. Published online 2011. Accessed November 25, 2022. https://www.wiley.com/en-us/Algorithms+for+Image+Processing+and+Computer+Vision%2C+2nd+Edition-p-9781118021880.
[29] S. Beucher, The watershed transformation applied to image segmentation, Scanning Microscopy-Supplement- (6) (1992) 299, 1992-299.
[30] S. Andreassen, F v. Jensen, K.G Olesen, Medical expert systems based on causal probabilistic networks, Int. J. Biomed. Comput. 28 (1–2) (1991) 1–30, https://doi.org/10.1016/0020-7101(91)90023-8.
[31] W. Wiegerinck, W. Burgers, B. Kappen, Bayesian networks, introduction and practical applications, Intelligent Syst. Reference Library 49 (2013) 401–431, https://doi.org/10.1007/978-3-642-36657-4_12.

[32] J.T.E. Richardson, The analysis of 2 × 2 contingency tables-Yet again, Stat. Med. 30 (8) (2011) 890, https://doi.org/10.1002/sim.4116. -890.
[33] L.P. Samuel, J.M. Balada-Llasat, A. Harrington, R. Cavagnolo, Multicenter assessment of gram stain error rates, J. Clin. Microbiol. 54 (6) (2016) 1442–1447, https://doi.org/10.1128/JCM.03066-15.
[34] T. Sandle, Assessing gram-stain error rates within the pharmaceutical microbiology laboratory, Eur. J. Parenteral and Pharmaceutical Sci. 25 (1) (2021), https://doi.org/10.37521/ejpps/25102.
[35] J. Guarner, C. Street, M. Matlock, L. Cole, F. Brierre, Improving Gram stain proficiency in hospital and satellite laboratories that do not have microbiology, Clin. Chem. Laboratory Med. (CCLM) 55 (3) (2017) 458–461, https://doi.org/10.1515/CCLM-2016-0556.
[36] S. Kotwal, P. Rani, T. Arif, J. Manhas, S. Sharma, Automated bacterial classifications using machine learning based computational techniques: architectures, challenges and open research issues, Archives of Computational Methods in Eng. 29 (4) (2022) 2469, https://doi.org/10.1007/S11831-021-09660-0.
[37] K.P. Smith, A.D. Kang, J.E. Kirby, Automated interpretation of blood culture gram stains by use of a deep convolutional neural network, J. Clin. Microbiol. 56 (3) (2018), https://doi.org/10.1128/JCM.01521-17.
[38] K.P. Smith, D.L. Richmond, T. Brennan-Krohn, H.L. Elliott, J.E. Kirby, Development of MAST: a microscopy-based antimicrobial susceptibility testing platform, SLAS Technol. 22 (6) (2017) 662–674, https://doi.org/10.1177/2472630317727721.
[39] M. Yang, K. Nurzynska, A.E. Walts, A. Gertych, A CNN-based active learning framework to identify mycobacteria in digitized Ziehl-Neelsen stained human tissues, Comput. Med. Imaging Graph 84 (2020), https://doi.org/10.1016/J.COMPMEDIMAG.2020.101752.
[40] P. Zawadzki, Deep learning approach to the classification of selected fungi and bacteria, in: Proceedings of 2020 IEEE 21st International Conference on Computational Problems of Electrical Engineering, CPEE, 2020, https://doi.org/10.1109/CPEE50798.2020.9238764. Published online September 1, 2020.
[41] B. Zieliski, A. Sroka-Oleksiak, D. Rymarczyk, A. Piekarczyk, M. Brzychczy-Woch, Deep learning approach to describe and classify fungi microscopic images, PLoS ONE 15 (6) (2020), https://doi.org/10.1371/JOURNAL.PONE.0234806.